Geophys. J. R. astr. Soc. (1974) **39**, 205–217.

Elastic Dislocations in a Layered Half-Space—I. Basic Theory and Numerical Methods

Dushan B. Jovanovich, Moujahed I. Husseini and Michael A. Chinnery*

(Received 1974 July 15)†

Summary

This paper is the first of a series that will examine the effect of earth structure on earthquake displacement, strain and tilt fields at the Earth's surface. Its purpose is to develop the numerical techniques to be applied in the papers that follow. A general computational procedure for the evaluation of the integral expressions for the surface displacements due to an arbitrary point dislocation source in a layered medium is described. It is shown to be rapid and inexpensive to use, and its accuracy appears to be entirely adequate for practical purposes.

Introduction

In recent years there has been a notable increase in the deployment of instruments such as geodimeters, strain and tiltmeters in active seismic regions. This has resulted in the accumulation of a considerable body of data relating to the permanent deformation of the Earth associated with earthquakes, fault movements and creep episodes. There are enough consistencies within these data that it is clear that they contain useful information both about the nature of the active tectonic processes and also (perhaps) about the structure of the Earth. However, the extraction of this information from the data has been severely limited by the oversimplified interpretation methods in general use.

These methods are all based on elastic dislocation theory, in which the source of the elastic fields is a displacement dislocation. The simplest model of an earthquake is obtained by placing such a source in a homogeneous elastic half-space. The resulting displacement and strain fields have been derived and discussed by Chinnery (1961), Maruyama (1964) and Press (1965), among others. This model is still used in most interpretations of displacement and strain data (e.g. Canitez & Toksöz 1972; Romig 1972; Mikumo 1973). However, the Earth is neither homogeneous nor a half space, and it is interesting to consider the effect of earth curvature and earth structure on the results obtained using the simple model.

As might be expected, the effect of earth curvature is very small in the near field. McGinley (1969) and Ben-Menahem, Singh & Solomon (1970) have compared the elastic fields in a homogeneous sphere to those in a homogeneous half space from the same source. Their results indicate that for shallow events the differences between the two cases are negligible at distances of less than 20°.

* Present address: Seismic Discrimination Group, Lincoln Laboratory, MIT, 42 Carleton Street, Cambridge, Massachusetts 02142.

† Received in original form 1974 April 30.

However, the effects of earth structure are potentially much more serious. This has become apparent from a number of studies. McGinley (1969) formulated the general solution for a point source in a multilayered medium. In particular, he studied the effects of a weak layer on the deformation fields of vertical strike-slip and dip-slip faults. Ben-Menahem & Gillon (1970) used the displacement expressions for a source in a single layer over a half space (Ben-Menahem & Singh 1968) to investigate the effect of a crustal layer on the displacement fields. Rybicki (1971), using the method of images, studied the effects of a single weak surface layer on the elastic fields on an infinite length strike-slip fault. Sato (1971) formulated the equations for a point source in a multilayered medium. He then calculated the response of the fields for the Gutenburg model with source in the surface layer, but there appear to be numerical instabilities in his computations. Sato & Matsu'ura (1973) using Sato's (1971) formulation calculated the displacement fields of a fault which spread over several layers in a multilayered earth. Chinnery & Jovanovich (1972) derived the expressions for an infinite length strike-slip fault in the presence of two layers over a half space, and investigated the effects of a soft layer at depth. All these studies have given insight into the consequences of earth layering but have limited the number of layers or constrained the source to lie in the first layer, with the exception of Sato & Matsu'ura (1973).

The present paper is the first in a series, in which we will investigate the effects of earth layering on the elastic fields of various dislocation sources. In this paper we describe the basic theory and numerical methods for evaluating the elastic fields associated with a buried source in a multilayered half space. In the three papers that follow, we will use these numerical methods to study, in turn, the point source, the line source and the source of finite size.

In order to resolve a discrepancy in the literature, we first give a résumé of the basic theory for a general Volterra-type point dislocation in a layered half space, following Singh (1970). We then describe a procedure for the numerical evaluation of the kernel functions in the integral expressions for the displacement field and method for approximating them so a rapid integration of the integral expressions can be performed. The method used to approximate the kernel functions is more general and accurate then the approximate expressions of the kernel functions previously used by McGinley (1969), Sato (1971) and Sato & Matsu'ura (1973) to evaluate the displacement fields. These methods place no restrictions on the location of the source nor on the number of layers.

Theory

The displacement field caused by an arbitrary shear dislocation located within an elastic medium may be expressed in terms of the solutions corresponding to four basic source types which satisfy the boundary conditions and the constitutive equations (see Ben-Menahem & Singh 1968a). In cylindrical co-ordinates (r, ε, z), with the source located at $(r = 0, z = h)$, the displacement components are

$$u_i = \sin\beta(u_i^3 \sin 2\gamma - u_i^2 \cos 2\gamma) + \cos\beta(u_i^1 \sin\gamma - u_i^4 \cos\gamma) \qquad (1)$$

where β and γ specify the orientation of the source, as shown in Fig. 1. If the source is considered to represent a fault, then β is the rake of the fault, γ is the dip of the fault, and the strike is taken along the x-axis while the slip is taken with respect to the hanging wall (Fig. 1).

The displacement u_i^1, u_i^2, u_i^3 are respectively the solutions for a vertical strike-slip source ($\beta = 0°, \gamma = 90°$), a vertical dip-slip source ($\beta = 90°, \gamma = 90°$) and a 45° dip-slip source ($\beta = 90°, \gamma = 45°$). The equation for the displacement u_i^4 is the same as that for u_i^2 with ε replaced by $(\varepsilon - \pi/2)$.

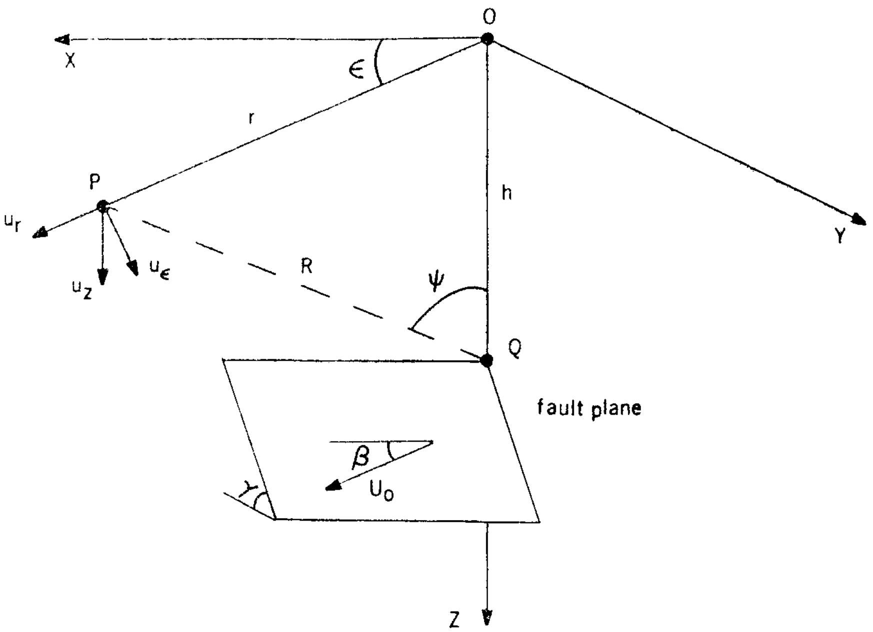

FIG. 1. Geometry of an arbitrary fault in cylindrical co-ordinates (r, ε, z) with origin O. P is the point of observation at a distance R from the source Q. The rake is β, the dip is γ, and U_0 is the displacement. The strike is taken along the x-axis.

The static displacement fields in a multilayered elastic half space may be obtained from the solution for an infinite medium by using the Thomson–Haskell matrix method (Thomson 1950; Haskell 1953). This procedure was formulated by Singh (1970), and we present merely a brief resume of his results.

Consider a semi-infinite elastic medium consisting of $(p-1)$ parallel, homogeneous and isotropic layers overlying a homogeneous, isotropic half space. The layers are numbered consecutively from the surface layer to the half space. The origin of the cylindrical co-ordinate system (r, ε, z) is placed at the free surface with the z-axis drawn into the medium. The nth layer is bounded by the interfaces z_{n-1} and z_n, has a thickness d_n and Lame constants μ_n and γ_n. The source is located in the sth layer and is at a depth h from the top interface (Fig. 2).

The vector displacement $\vec{u}_n$, in the nth layer, satisfies the Navier equation of static elasticity for an infinite medium,

$$\{\nabla^2 + (1+\lambda_n/\mu_n)\,\mathrm{grad\,div}\} \quad \vec{u}_n = 0. \tag{2}$$

The three independent solutions of this equation are given by Morse & Feshback (1953) and Ben-Menahem & Singh (1968b). These are:

$$\left.\begin{aligned} \vec{N}_{nm}{}^{\pm} &= \exp(\pm kz)(\pm\vec{P}_m + \vec{B}_m) \\ \vec{F}_{nm}{}^{\pm} &= \exp(\pm kz)(\pm 1 - 2\delta_n kz)\vec{P}_m - \exp(\pm kz)(1 \pm 2\delta_n kz)\vec{B}_m \\ \vec{M}_{nm}{}^{\pm} &= \exp(\pm kz)\vec{C}_m \end{aligned}\right\} \tag{3}$$

where

$$\delta_n = (\lambda_n + \mu_n)/(\lambda_n + 3\mu_n)$$

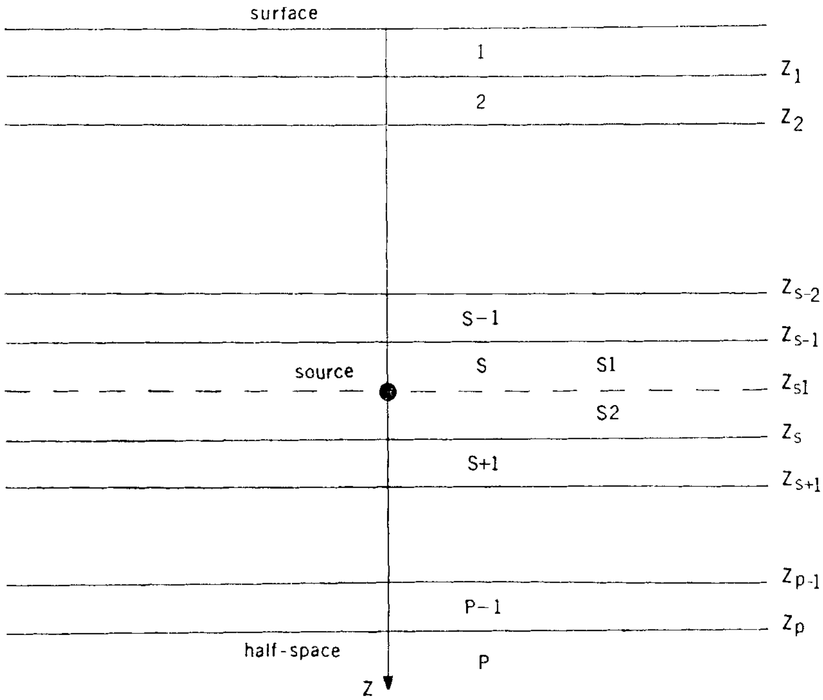

FIG. 2. Multilayered half space with $(p-1)$ layers. The source is located at Z_{s1}, in the s-th layer at a depth h from the interface Z_{s-1}. The half-space is at a depth H from the surface.

and

$$\vec{P}_m = \vec{e}_z\, J_m(kr) \exp(Im\varepsilon)$$

$$\vec{B}_m = (\vec{e}_r\, \partial/\partial kr + \vec{e}_\varepsilon\, (1/kr)\partial/\partial\varepsilon) J_m(kr) \exp(Im\varepsilon)$$

$$\vec{C}_m = (\vec{e}_r\, (1/kr) \frac{\partial}{\partial\varepsilon} - \vec{e}_\varepsilon \partial/\partial kr) J_m(kr) \exp(Im\varepsilon).$$

The surface displacements may be deduced by matching at the interfaces the coefficients of the general solutions by the Thomson–Haskell matrix method. The integral expressions for displacement for the three sources mentioned above are:

(i) for a vertical strike-slip source,

$$\left.\begin{aligned} u_r &= -\int_0^\infty [(1/i)y_{12}(0)(\partial/\partial kr)J_2(kr) + z_{12}(0)(2/kr)J_2(kr)]\, k\,dk \sin 2\varepsilon \\ u_\varepsilon &= -\int_0^\infty [(1/i)y_{12}(0)(2/kr)J_2(kr) + z_{12}(0)(\partial/\partial kr)J_2(kr)]\, k\,dk \cos 2\varepsilon \\ u_z &= -\int_0^\infty (1/i)x_{12}(0)J_2(kr)\, k\,dk \sin 2\varepsilon \end{aligned}\right\} \quad (4)$$

(ii) for a vertical dip-slip source,

$$\left.\begin{aligned} u_r &= -\int_0^\infty [(1/i)y_{11}(0)(\partial/\partial kr)J_1(kr)+z_{11}(0)(1/kr)J_1(kr)]\,kdk\sin\varepsilon \\ u_\varepsilon &= -\int_0^\infty [(1/i)y_{11}(0)(1/kr)J_1(kr)+z_{11}(0)(\partial/\partial kr)J_1(kr)]\,kdk\cos\varepsilon \\ u_z &= -\int_0^\infty (1/i)x_{11}(0)J_1(kr)\,kdk\sin\varepsilon \end{aligned}\right\} \tag{5}$$

(iii) for a 45° dip-slip source,

$$\left.\begin{aligned} u_r &= -\int_0^\infty \Big(y_{10}(0)J_1(kr)+(1/i)z_{12}(0)(2/kr)J_2(kr) \\ &\qquad -y_{12}(0)(\partial/\partial kr)J_2(kr)\Big)\cos 2\varepsilon\Big)\,kdk \\ u_\varepsilon &= -\int_0^\infty [(2/kr)y_{12}(0)J_2(kr) \\ &\qquad -(1/i)z_{12}(0)(\partial/\partial kr)J_2(kr)]\,kdk\sin 2\varepsilon \\ u_z &= \int_0^\infty \big(x_{10}(0)J_0(kr)+x_{12}(0)J_2(kr)\cos 2\varepsilon\big)\,kdk. \end{aligned}\right\} \tag{6}$$

Another important seismic source is the centre of compression; and the integral expressions for the corresponding displacements are,

$$\left.\begin{aligned} u_r &= -\int_0^\infty y_{10}(0)J_1(kr)\,kdk \\ u_\varepsilon &= 0 \\ u_z &= \int_0^\infty x_{10}(0)J_0(kr)\,kdk. \end{aligned}\right\} \tag{7}$$

The kernel functions $x_{1m}(0)$, $y_{1m}(0)$ and $z_{1m}(0)$ are given by:

$$\left.\begin{aligned} x_{1m}(0) &= \big(E|_{13}{}^{14}(F_m)_3+E|_{31}{}^{13}(F_m)_4\big)/(E|_{13}{}^{34})-(F_m)_1 \\ y_{1m}(0) &= \big(E|_{13}{}^{24}(F_m)_3+E|_{31}{}^{23}(F_m)_4\big)/(E|_{13}{}^{34})-(F_m)_2 \\ z_{1m}(0) &= \big(E_{11}{}^{L}(F_m{}^{L})_2\big)/E_{21}{}^{L}-(F_m{}^{L})_1 \end{aligned}\right\} \tag{8}$$

where

$$\left.\begin{aligned} E|_{kl}{}^{ij} &= E_{ik}\,E_{jl}-E_{il}\,E_{jk} \\ (E) &= (a_1)(a_2)\ldots(a_{s-1})(a_s)\ldots(a_{p-1})\big(Z_p(H)\big) \\ (E^L) &= (a_1{}^L)(a_2{}^L)\ldots(a_{s-1}{}^L)(a_s{}^L)\ldots(a_{p-1}{}^L)\big(z_p(H)^L\big) \\ (F_m) &= (a_1)(a_2)\ldots(a_{s-1})(a_{s1})(D_m) \\ (F_m{}^L) &= (a_1{}^L)(a_2{}^L)\ldots(a_{s-1}{}^L)(a_{s1}{}^L)(D_m{}^L) \end{aligned}\right\} \tag{9}$$

where (a_n) and $(a_n{}^L)$ are the layer matrices and the subscript denotes the layer number. The $s1$ subscript refers to the portion of the source layer which lies between the source and the interface above it. The $(Z_p(H))$ and $(Z_p(H)^L)$ are the coefficient matrices of the half space and the (D_m) and $(D_m{}^L)$ are the source vectors which are determined by the discontinuities in the displacements and stresses. All of these matrices are listed in the Appendix. The vectors (D_m) and $(D_m{}^L)$ are listed for the four basic source types (Steketee 1958; Singh 1970).

Ben-Menahem & Singh (1968a) derived the expressions for the displacements due to a buried source for the case of a single layer overlying a half space. Ben-Menahem & Gillon (1970), using these results, numerically evaluated the static surface displacements. Some of the expressions of Ben-Menahem & Singh (1968a) differ from those of Singh (1970). The (E) matrices and the (F_m) vectors for a single layer overlying the half space are from (9),

$$\left.\begin{aligned}(E) &= (a_1)(Z_p(H))\\ (E^L) &= (a_1{}^L)(z_p(H)^L)\\ (F_m) &= (a_{s1})(D_m)\\ (F_m{}^L) &= (a_{s1}{}^L)(D_m{}^L).\end{aligned}\right\} \qquad (10)$$

By performing the matrix manipulations and substituting into equations (4) and (5), we should obtain Ben-Menahem & Singh's equations (11–56) and (11–58). A difference in $\eta_6{}^-$ and $\eta_2{}^\pm$ terms defined in their equations (11–57) and (11–59) is evident. The equations should be,

$$\left.\begin{aligned}\eta_6{}^- &= -Z_4+\delta Z_1(1-2kH)(1+2\delta k(H-h))\\ \eta_2{}^\pm &= \mp Z_4-\delta_2{}^2 Z_1(1\pm 2kH)(1+2k(H-h))\end{aligned}\right\} \qquad (11)$$

where the above terms are defined in their equations (11–52) and (11–43). These differences imply their equations for u_z for a vertical strike-slip source, and all three displacements in vertical dip-slip source are incorrect. Though these errors appear in both the results of Ben-Menahem & Singh (1968a), and Ben-Menahem & Gillon (1970), they may be a misprint.

Numerical methods

One of the major difficulties in dealing with the integral expressions for displacement is the evaluation of the kernel functions. The reduction of these functions to an algebraic closed form is extremely tedious and they are difficult to evaluate numerically since they involve matrix products of highly disproportionate terms. In order to avoid this problem the (a_n) matrix may be decomposed into the sum of four matrices,

$$(a_n) = \exp(-kd_n)(A_n{}^1)+\exp(-kd_n)k(A_n{}^2) +\exp(+kd_n)(A_n{}^3)+\exp(+kd_n)k(A_n{}^4) \qquad (12)$$

where the $A_n{}^m$ matrices contain only constant coefficients. The $(Z_p(H))$ is similarly treated. In this fashion the (E) matrix may be rewritten as the product of constant matrices while all the exponentials and powers of k are carried outside the appropriate matrix product. The final form of the (E) matrix becomes,

$$(E) = \sum_{l=1}^{L} \exp(-kD_l) \sum_{n=0}^{N} (e)_{nl}\, k^n \qquad (13)$$

where D_l are the exponential arguments resulting from the product of the 'factored-out' exponentials. $(e)_{nl}$ are the coefficient matrices arising from the matrix product of the (A_n^m) and $(Z_p(H))$ matrices associated with the nth power of k and the lth exponential argument. N is $p+1$ and L is 2^p. The (F_m) vector may be similarly treated once the appropriate source vector (D_m) is selected.

The numerators of the kernel functions are formed from the second order subdeterminants of the (E) matrix multiplied by the appropriate (F_m) term. The (F_m) term introduces positive-argument exponentials which cancel out in the final form but may not do so numerically due to round-off error. These terms are cancelled artificially to avoid any numerical instability. The final form of the kernel functions $x_{1m}(0)$ and $y_{1m}(0)$ is a ratio of finite series of exponentials multiplied by polynomials,

$$\frac{\sum_{n=1}^{N} \exp(-kD_n) \sum_{m=0}^{M} a_{mn}k^m}{\sum_{n=1}^{P} \exp(-kC_n) \sum_{m=0}^{Q} b_{mn}k^m} \tag{14}$$

where N is $2^{2(p-1)+s}$, M is $2p+s-1$, P is $2^{2(p-1)}$ and Q is $2p-1$ (p is the number of layers plus one and s is the source layer number).

The (a_n^L), $(Z_p(H)^L)$, and (F_m^L) matrices are more easily treated since they do not involve polynomials of k. The (a_n^L) matrix is decomposed into,

$$(a_n^L) = \exp(-kd_n)(A_n^{1L}) + \exp(+kd_n)(A_n^{2L}) \tag{15}$$

and the final form of the $z_{1m}(0)$ kernel function is,

$$\frac{\sum_{i=1}^{I} a_i \exp(-kA_i)}{\sum_{j=1}^{J} b_j \exp(-kB_j)} \tag{16}$$

where I is 2^{p+s-1} and J is 2^{p-1}.

This procedure for evaluating the kernel functions is stable. We believe the oscillations in Sato's (1971) numerical evaluation of this kernel functions, which are similar to ours, may be due to numerical instability (his Figs 3–5). The oscillations, however, do not appear in Sato & Matsu'ura's (1973) paper.

The occurrence of the polynomial-exponential series in the denominator of the kernel functions renders exact analytical integration of the displacement integral expressions impossible. However, a more detailed examination of the denominator of the kernel functions (equation (14)) yields the interesting result that it may be expressed in the form

$$1/\left(b_{01} + \sum_{n=2}^{P} \exp(-kC_n) \sum_{m=0}^{Q} b_{mn}k^m\right). \tag{17}$$

This is true because $x_{1m}(0)$ and $y_{1m}(0)$ have a second-order subdeterminant in their denominator which may be written as,

$$E|_{13}{}^{34} = a_1|_{mn}{}^{34}\, a_2|_{op}{}^{mn} \ldots a_{p-1}|_{uv}{}^{st}\, Z_p(H)|_{13}{}^{uv} \tag{18}$$

where the summed pairs of indices are only distinct pairs (i.e. $m > n$, see Dunkin 1965). The second-order subdeterminants associated with the polynomial coefficients of the zero-argument exponential are identically zero with the exception of the zero-power coefficient ($b_{01} \neq 0$; $b_{i1} = 0$, $i = 1, Q$).

This form of the denominator of the kernel functions allows the use of a method suggested by Sneddon (1951) which was successfully applied to a single layer over a half space by Ben-Menahem & Gillon (1970). This method consists chiefly in approximating the denominator by a truncated binomial series expansion and then fitting the reminder of the series with a sum of exponential-polynomial terms using the method of least squares. Thus the denominator of the kernel functions $x_{1m}(0)$ and $y_{1m}(0)$ in (17) takes the new form,

$$(1/b_{01})\left(1-\sum_{n=2}^{P}\exp(-kC_n)\sum_{m=0}^{Q}(b_{mn}/b_{01})k^m\right)+\sum_{j=0}^{R}r_j k^j\exp(-kS_j) \tag{19}$$

where the r_j and S_j are found by a least-square approximation. $z_{1m}(0)$ is similarly treated. By multiplying the exact numerator series by the approximated inverse denominator series, the kernel functions become a finite sum of exponentials multiplied by polynomials. The displacement integral expressions will now take the form,

$$u(r)=\sum_l\sum_n a_{ln}\int_0^\infty k^n\exp(-kD_l)J_p(kr)dk. \tag{20}$$

This is the Lipshitz–Hankell integral and its exact quadrature may be found (Erdelyi 1954). The integral may be reduced to a simpler form following Ben-Menahem & Gillon (1970). Introducing spherical co-ordinates (Fig. 1),

$$\left.\begin{aligned} D &= R\cos\psi \\ r &= R\sin\psi \end{aligned}\right\} \tag{21}$$

and denoting

$$F_{nm}(r)=\int_0^\infty k^n\exp(-kD)J_m(kr)dk \tag{22}$$

then from Watson (1944),

$$\begin{aligned} F_{nm}(R,\cos\psi) &= ((n-m)!/R^{n+1})P_n^m(\cos\psi) \qquad n\geqslant m \\ &= \tan\tfrac{1}{2}\psi K_n^m(\cos\psi)/R^{n+1}\ m,n>0 \end{aligned} \tag{23}$$

where $P_n^m(\cos\psi)$ is the associated Legendre polynomial and K_n^m is given by the recursion formulas (Ben-Menahem & Gillon 1970),

$$\left.\begin{aligned} K_0^m &= 1 \\ K_1^m &= m+\cos\psi \\ K_n^m &= (2n-1)\cos\psi K_{n-1}^m+(m+n-1)(m-n+1)K_{n-2}^m. \end{aligned}\right\} \tag{24}$$

Test of numerical accuracy

To establish the numerical accuracy of the method described here, an arbitrarily chosen model was studied using different numerical schemes. This model consisted of three layers overlying a half space with rigidity contrasts of 0·1, 1·0, 0·1, 1·0 and thicknesses in kilometres of 5, 30, 5 and infinity, respectively. The Poisson ratio was selected to be 0·25 and a vertical strike-slip point source was placed at a depth of 20 km. The source had a 1-m displacement and a surface area of one square km (Fig. 3, insert). This model is of particular interest to DC seismology since it incorporates both a weak surface layer and a thin partial melt zone.

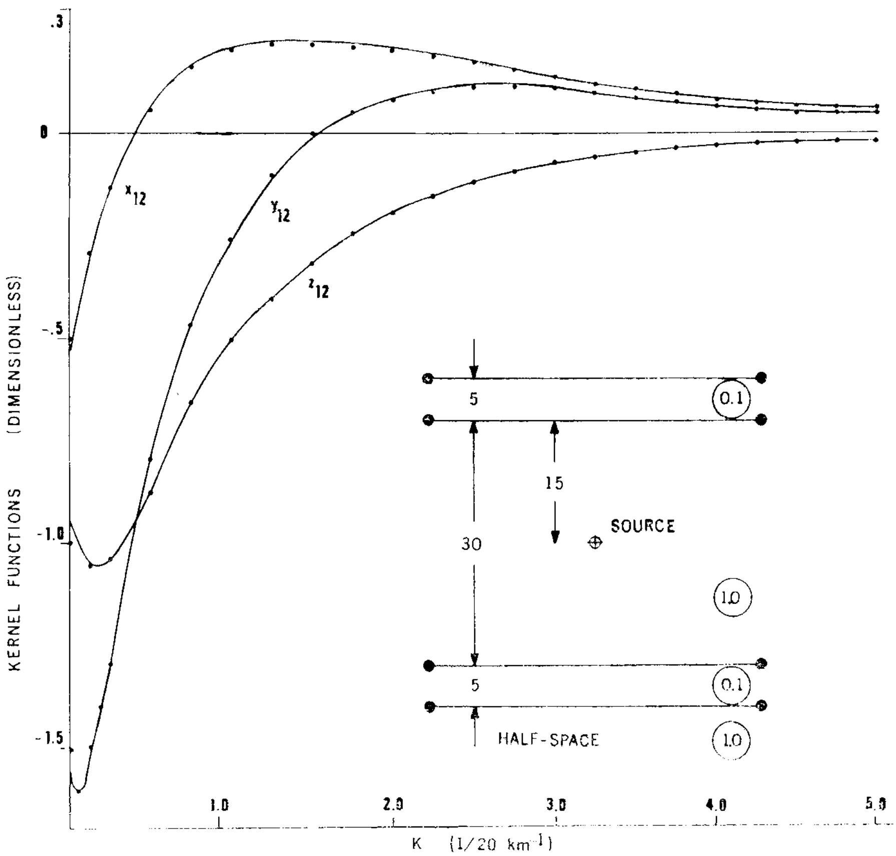

FIG. 3. Approximations of the three kernel functions $x_{12}(0)$, $y_{12}(0)$ and $z_{12}(0)$ for the three-layer earth model with a weak surface layer and a thin partial melt zone (see insert). The k-axis is scaled by a factor of 20.

The kernel functions $x_{12}(0)$ and $y_{12}(0)$ have 54 exponential terms in the numerator and 32 in the denominator. The $z_{12}(0)$ kernel function had four exponential terms in the numerator and six in the denominator. After expanding the denominators in a truncated binomial series, the difference between the denominator and its binomial expansion was fit by a sum of exponentials using least squares. For $x_{12}(0)$ and $y_{12}(0)$ a single exponential was sufficient to yield a maximum relative error of 5·21 per cent and an average relative error of 1·36 per cent. The $z_{12}(0)$ function was fit with the sum of two exponentials and its maximum relative error was 4·04 per cent and the average relative error was 0·174 per cent. The relative error decreased sharply as k approached about 5·0 (Fig. 3). With a four-layer Gutenberg Earth model, which had less marked rigidity contrasts, the kernel functions were approximated in a similar fashion to within 1 per cent maximum relative error.

Upon reducing the integral expressions for the displacements to the form of equation (20), an exact quadrature is possible. The radial and vertical displacements were evaluated on a digital computer (IBM 360-67) and required 5 s for each value of r. The integral expressions were also evaluated using a numerical quadrature scheme (J. Gregory) where the area of the integral is evaluated between each of the zero-crossings of the Bessel functions. The method was programmed to proceed with the summing of areas until the final integral contribution of the zero-crossing was less than 0·1 per cent. At $r = 60$ km, with 80 values of the integrand between zero-crossings, the method required nearly 2 min.

Table 1

r (km)	Radial displacement (m) Numerical quadrature	No. of points*	Approximation method	Rel. error (%)	Vertical displacement (m) Numerical quadrature	No. of points	Approximation method	Rel. error (%)
20	$0\cdot174\times10^{-3}$	80	$0\cdot176\times10^{-3}$	1·1	$-0\cdot898\times10^{-4}$	80	$-0\cdot914\times10^{-4}$	1·7
60	$0\cdot667\times10^{-4}$	80	$0\cdot669\times10^{-4}$	0·3	$-0\cdot679\times10^{-5}$	80	$-0\cdot676\times10^{-5}$	−0·4
180	$0\cdot869\times10^{-5}$	20	$0\cdot882\times10^{-5}$	1·4	$0\cdot994\times10^{-6}$	20	$0\cdot983\times10^{-6}$	−1·1
380	$0\cdot156\times10^{-5}$	10	$0\cdot168\times10^{-5}$	7·1	$0\cdot418\times10^{-6}$	10	$0\cdot412\times10^{-6}$	−1·5

* No of points refers to the number of integrand values between zero-crossings of the Bessel functions.

A comparison of the results of the two schemes at various distances is presented in Table 1. That reasonably close results were obtained by the two independent schemes is quite remarkable since they are both subject to numerical error. The larger relative error at $r = 180$ and 380 km is due to the limited number of integrand values per zero-crossing selected for the numerical quadrature. This limitation is due to the drastically increasing number of zero-crossings of the Bessel functions needed to converge to an accurate solution at large r. Thus the computation time for the numerical quadrature will increase dramatically as r becomes large while the approximation method maintains a constant computation time at all values of r.

Summary

In this study, we have established a procedure for the evaluation of the surface displacements caused by an arbitrary point source in a layered medium. The strains and tilts may also be obtained from this procedure since their integral expressions are very similar to those of the displacements. The results may be extended to evaluate the elastic fields of a finite and infinite fault in a layered medium.

The computational procedure is quite general, inexpensive and accurate in dealing with layered media. The basic theory is attractive since the mathematical formulation is presented in a concise matrix form. The inherent numerical difficulties of the Thomson–Haskell matrix formulation have been circumvented by algebraic manipulations. We can, therefore, obtain the exact forms of the kernel functions in the displacement integral expressions. By expanding the denominators of the kernel functions in a truncated binomial series and fitting the remainders by least squares, we can obtain an exact quadrature of the integral expressions.

In later papers in this series, these techniques will be applied to the evaluation of the effect of earth structure on earthquake displacement and strain fields measured at the Earth's surface.

Acknowledgments

The authors are grateful to Dr Michael J. Randall for many helpful discussions. This research was supported by National Science Foundation Grant GA-18870.

Department of Geological Sciences,
Brown University,
Providence, Rhode Island 02912

References

Ben-Menahem, A. & Gillon, A., 1970. Crustal deformation by earthquakes and explosions, *Bull. seism. Soc. Am.*, **60,** 193–215.

Ben-Menahem, A. & Singh, S. J., 1968a. Multipolar elastic fields in a layered half-space, *Bull. seism. Soc. Am.*, **58,** 1519–1572.

Ben-Menahem, A. & Singh, S. J., 1968b. Eigenvector expansions of Green's dyads with applications to geophysical theory, *Geophys. J. R. astr. Soc.*, **16,** 417–452.

Ben-Menahem, A., Singh, S. J. & Solomon, F., 1970. Deformation of an homogeneous earth model by finite dislocations, *Rev. geophys. Space Phys.*, **8,** 591–632.

Canitez, N. & Toksöz, M. N., 1972. Static and dynamic study of earthquake mechanism: San Fernando earthquake, *J. geophys. Res.*, **77,** 2583–2594.

Chinnery, M. A., 1961. The deformation of the earth around surface faults, *Bull. seism. Soc. Am.*, **51,** 355–372.

Chinnery, M. A. & Jovanovich, D. B., 1972. Effect of earth layering on earthquake displacement fields, *Bull. seism. Soc. Am.*, **62,** 1629–1639.

Dunkin, J. W., 1965. Computation of modal solutions in layered elastic media at high frequencies, *Bull. seism. Soc. Am.*, **55,** 335–358.

Erdelyi, A., Ed., 1954. *Tables of integral transforms*, Vol. II, p. 28, McGraw–Hill Book Co., Inc.

Haskell, A., 1953. The dispersion of surface waves on a multilayered media, *Bull. seism. Soc. Am.*, **43,** 17–34.
Maruyama, T., 1964. Statical elastic dislocations in an infinite and semi-infinite medium, *Bull. earthq. Res. Inst.*, **42,** 289–368.
McGinley, J. R., 1969. *A comparison of observed permanent tilts and strains due to earthquakes with those calculated from displacement dislocations in elastic earth models*, unpublished Ph.D. Thesis, C.I.T.
Mikumo, T., 1973. Faulting process of San Fernando earthquake of February 9, 1971 inferred from static and dynamic near-field displacements, *Bull. seism. Soc. Am.*, **63,** 249–270.
Morse, P. M. & Feshbach, H., 1946. *Methods of theoretical physics*, Part II, p. 979, McGraw–Hill Book Co., Inc.
Press, F., 1965. Displacements, strains and tilts at tele-seismic distances, *J. geophys. Res.*, **70,** 2395–2412.
Romig, P. R., 1972. Interpretation of strain data—CANNIKIN nuclear test, *Bull. seism. Soc. Am.*, **62,** 1473–1478.
Rybicki, K., 1971. The elastic residual field of a very long strike-slip fault in the presence of a discontinuity, *Bull. seism. Soc. Am.*, **61,** 79–92.
Sato, R., 1971. Crustal deformation due to a dislocation in a multilayered medium, *J. phys. Earth*, **19,** 31–46.
Sato, R. & Matsu'ura, M., 1973. Static deformations due to the fault spreading over several layers in a multilayered medium, Part I: Displacement, *J. Phys. Earth.*, **21,** 227–249
Singh, S. J., 1970. Static deformation of a multilayered half-space by internal sources, *J. geophys. Res.*, **75,** 3257–3263.
Sneddon, I. N., 1951. *Fourier transforms*, 476–479, McGraw–Hill Book Co.
Steketee, J. A., 1958. On Volterra's dislocation in a semi-infinite elastic medium, *Can. J. Phys.*, **36,** 192–205.
Thomson, W. T., 1950. Transmission of elastic waves through a stratified medium, *J. appl. Phys.*, **21,** 89–93.
Watson, G. N., 1944. *A treatise on the theory of Bessel functions*, Cambridge University Press.

Appendix

The elements of the $Z_p(H)$ matrix are,

$$\left.\begin{aligned}
(11) &= -(21) = -\exp(-kH)\\
(12) &= (22) = \exp(kH)\\
(13) &= -(1+2\delta_p kH)\exp(-kH)\\
(14) &= (1-2\delta_p kH)\exp(-kH)\\
(23) &= -(1-2\delta_p kH)\exp(-kH)\\
(24) &= -(1+2\delta_p kH)\exp(kH)\\
(31) &= -(41) = \mu_p \exp(-kH)\\
(32) &= (42) = \mu_p \exp(kH)\\
(33) &= \mu_p \delta_p (1+2kH)\exp(-kH)\\
(34) &= \mu_p \delta_p (1-2kH)\exp(kH)\\
(43) &= \delta_p \mu_p (1-2kH)\exp(-kH)\\
(44) &= -\mu_p \delta_p (1+2kH)\exp(kH)
\end{aligned}\right\} \quad (A1)$$

the elements of the $Z_p(H)^L$ matrix are,

$$\left.\begin{aligned}(11) &= \exp(-kH)\\ (12) &= \exp(kH)\\ (21) &= -\mu_p \exp(-kH)\\ (22) &= \mu_p \exp(kH)\end{aligned}\right\} \quad \text{(A2)}$$

the elements of the $a_n(2\mu(1+\delta))$ matrix are,

$$\left.\begin{aligned}(11) &= (33) = 2\mu\big((1+\delta)\cosh kd - 2\delta kd \sinh kd\big)\\ (12) &= -(43) = 2\mu\big((1-\delta)\sinh kd - 2\delta kd \cosh kd\big)\\ (13) &= 4(-\sinh kd + \delta kd \cosh kd)\\ (14) &= -(23) = 4\delta\, kd \sinh kd\\ (21) &= -(34) = 2\mu\big((1-\delta)\sinh kd + 2\delta \cosh kd\big)\\ (22) &= (44) = 2\mu\big((1+\delta)\cosh kd + 2\delta kd \sinh kd\big)\\ (24) &= -4(\sinh kd + \delta kd \cosh kd)\\ (31) &= 4\mu^2(-\sinh kd + kd \cosh kd)\\ (32) &= -(41) = 4\mu^2\, \delta kd \sinh kd\\ (42) &= -4\mu^2\, \delta(\sinh kd + kd \cosh kd)\end{aligned}\right\} \quad \text{(A3)}$$

where the subscript has been dropped for μ_n, δ_n, and d_n. The elements of $a_n{}^L$ are,

$$\left.\begin{aligned}(11) &= (22) = \cosh kd\\ (12) &= -\mu^{-1} \sinh kd\\ (21) &= -\mu \sinh kd\end{aligned}\right\} \quad \text{(A4)}$$

where subscript n has been dropped for μ_n and d_n.

The four elementary source vectors D_m and $D_m{}^L$ are for vertical strike-slip $(i, j) = (1, 2)$,

$$(D_2)_4 = \mu_s \chi i \qquad (D_2{}^L)_2 = 2\mu_s \chi \quad \text{(A5)}$$

vertical dip-slip $(i, j) = (2, 3)$,

$$(D_1)_2 = -2\chi i \qquad (D_1{}^L)_1 = -2\chi \quad \text{(A6)}$$

45° dip-slip $(i, j) = \tfrac{1}{2}((2, 2)-(3, 3))$,

$$\left.\begin{aligned}(D_0)_1 &= 2\chi(\delta_s - 1)/(\delta_s + 1)\\ (D_2)_4 &= \tfrac{1}{2}\mu_s \chi\\ (D_0)_4 &= \tfrac{1}{2}\mu_s \chi(7\delta - 1)/(\delta_s + 1) \qquad (D_2{}^L)_2 = -\mu_s \chi i\end{aligned}\right\} \quad \text{(A7)}$$

centre of compression $(i, j) = (1, 1)+(2, 2)+(3, 3)$,

$$\left.\begin{aligned}(D_0)_1 &= 2\chi(7\delta_s - 1)/(\delta_s + 1)\\ (D_0)_4 &= 2\mu_s \chi(7\delta_s - 1)/(\delta_s + 1)\end{aligned}\right\} \quad \text{(A8)}$$

where $\chi = U_0\, dS/4\pi$ and U_0 is the average dislocation over the surface area dS. Subscript s refers to the source layer.